AIIM

Association for Information and Image Management

1100 Wayne Avenue, Suite 1100
Silver Spring, Maryland 20910

301/587-8202

Centimeter

Inches

1 of 1

NUCLEAR STRUCTURE DEPENDENCE OF THE SUB-BARRIER FUSION ENHANCEMENT FOR NUCLEI IN THE MASS 90 REGION

K. E. Rehm, C. L. Jiang, H. Esbensen, B. Crowell, J. Gehring, B. Glagola, W. Kutschera, Y. Liang, M. D. Rhein, K. Teh, A. H. Wuosmaa
Physics Division
Argonne National Laboratory
Argonne, Illinois 60439 USA

Abstract

Cross sections for evaporation residue production have been measured for the systems ^{58,64}Ni + ^{78,86}Kr and ^{58,64}Ni + ^{92,100}Mo at energies below and above the Coulomb barrier. Coupled-channels calculations including one-and two-phonon excitations of low-lying collective states in the projectile and target give excellent agreement for systems involving the closed shell nuclei ^{86}Kr and ^{92}Mo. Fusion cross sections for systems involving the transitional nuclei ^{78}Kr and ^{100}Mo, however, show an additional fusion enhancement indicating the need for the inclusion of higher order processes in the calculations.

1. Introduction

The enhancement of heavy-ion induced fusion reactions at sub-barrier energies has been successfully explained by a variety of microscopic and macroscopic models[1-3]. Coupled-channels calculations including inelastic excitations of low-lying states have been able to provide a quantitative understanding of the large fusion probabilities, especially for systems involving nuclei with $A \leq 32$. While for many systems excellent agreement between theory and experiment has been achieved, some projectile-target combinations4 (e.g. ^{58}Ni + ^{64}Ni) have measured cross sections exceeding the theoretical predictions by up to a factor of 10. More complete coupled-channel calculations, including other processes such as quasielastic few particle transfers have been attempted to obtain a better agreement between theory and experiment. The effect of these additional channels, however, was found to be relatively small[4,5]. In order to shed some more light on other possible causes for the large sub-barrier fusion enhancement, such as the effects of the intrinsic nuclear structure of the colliding nuclei, we have studied fusion in several systems in the mass A=90 region. The influence of permanent deformation on the fusion probability at low energies is well established and has been studied e.g. in systems involving spherical and deformed Sm isotopes. Nuclei in the mass 90 region do not show permanent deformation but instead change from spherical (^{92}Mo and ^{86}Kr) to transitional nuclei (^{78}Kr, ^{100}Mo). In this contribution the results of evaporation residue production for ^{58,64}Ni + ^{78,86}Kr and ^{58,64}Ni +

^{92,100}Mo will be discussed.

2. Experimental Details

The experiments were performed with ^{58,64}Ni and ^{78,86}Kr beams for the Ni + Mo and Ni + Kr systems, respectively. The beams were obtained from the superconducting linear accelerator ATLAS at ANL. The targets consisted of Ni and Mo foils with typical thicknesses between 200 and 400 $\mu g/cm^2$. To separate the evaporation residues, which are emitted at very forward angles, from the the elastically scattered beam particles the method of a gas-filled magnet was utilized. Due to momentum conservation and because beam and residues have similar charge state distributions no spatial separation of the two components can be achieved with a magnetic field if the particles move in vacuum. If the magnetic field region is filled with a gas of sufficient pressure (typically N_2 at 0.2-1 Torr), however, the ions experience charge-changing collisions and travel with an average charge state $\bar{q}$. Since $\bar{q}$ depends on the ion velocity v and the nuclear charge Z to first order as $q \sim v \times Z^{\gamma}$ the average magnetic rigidity $B\rho = mv/\bar{q} \sim m/Z^{\gamma}$ is independent of the velocity v. This velocity focussing property of a gas-filled magnet thus results in a large energy acceptance for the spectrometer.

An Enge Split-Pole spectrograph[6] was used for the measurements with an x-y position sensitive parallel grid avalanche counter in its focal plane. Details of the detector and the complete experimental setup are given in Ref.[7]. Together with a time-of-flight (TOF) measurement utilizing the pulsed beam capabilities of ATLAS, good separation between evaporation residues and elastically scattered particles was achieved. An example for the system ^{58}Ni + ^{100}Mo measured at E_{lab}=248.7 MeV and 217.2 MeV and Θ_{lab}=3° and 1.2°, respectively, is shown in Fig.1. No corrections for charge-state distribution or acceptance efficiency are needed for this technique. Similar results are obtained for the ^{58,64}Ni + ^{78,86}Kr case. Angular distributions have been measured between 1.2° and 7° at every other bombarding energy for the various systems. At the intermediate energies cross sections were measured at 1.4°, 1.7° and 3°, respectively. The shape of the angular distributions was approximated by the sum of two Gaussians, whose widths varied slowly with bombarding energy. The cross sections of the evaporation residues were normalized to elastic scattering yields, with the absolute scattering angle determined by measurements on either side of the beam.

3. Discussion

3.1 Experimental Results

The angle-integrated cross sections for the evaporation residues measured for ^{58}Ni + ^{78,86}Kr and ^{92,100}Mo are shown in Fig.2 as function of the center-of-mass energy. The

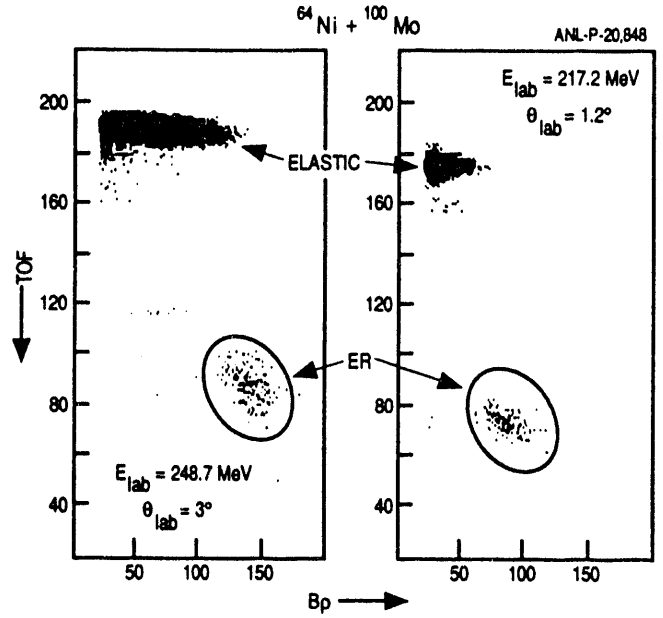

Figure 1: Time-of-Flight (TOF) vs. Magnetic Rigidity (Bρ) measured with the gas-filled magnet technique for the system ^{64}Ni + ^{100}Mo at E_{lab}=248.7 MeV and 217.2 MeV.

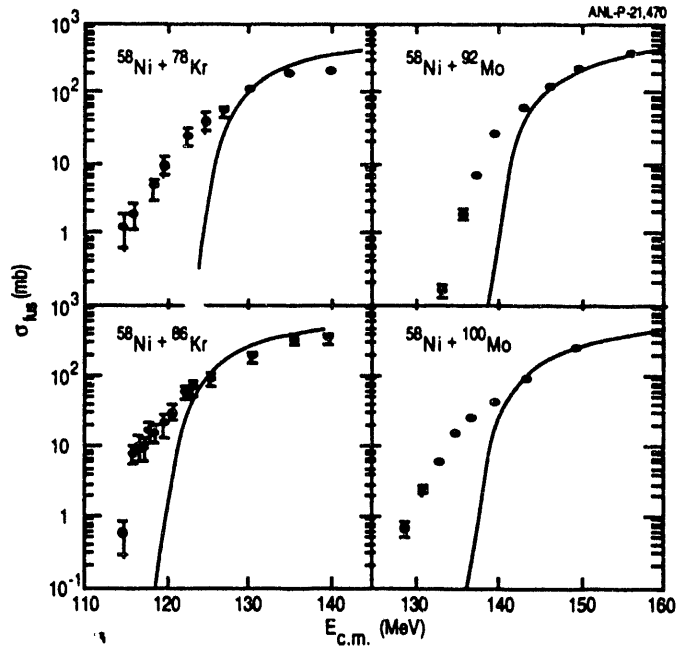

Figure 2: Excitation functions measured for the systems ^{58}Ni + ^{78,86}Kr and ^{92,100}Mo. The solid lines are the result of one-dimensional barrier penetration calculations.

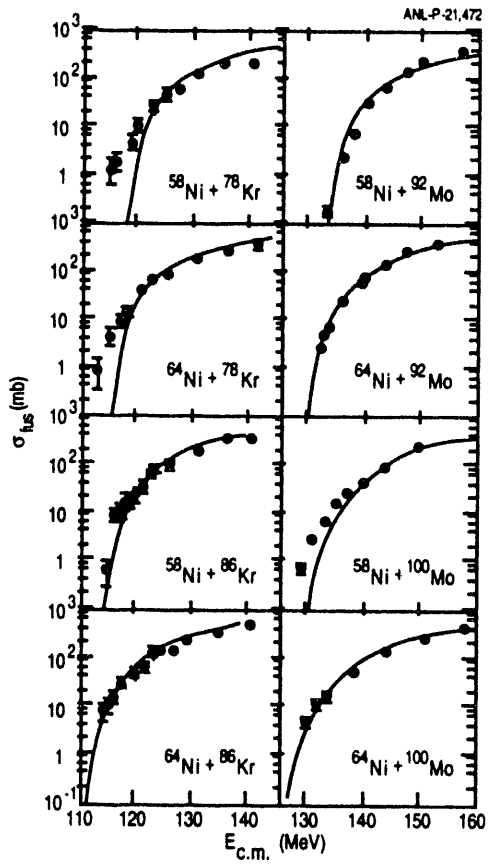

Figure 3: Excitation functions for the systems ^{58,64}Ni + ^{78,86}Kr and ^{92,100}Mo. The solid lines are the results of coupled-channels calculations including one-and two-phonon excitations of low-lying states in projectile and target. See text for details.

data have been corrected for the energy loss in the target, taking the strong energy dependence of the cross sections at low bombarding energies into account. The solid lines are the results of the one-dimensional barrier penetration model which underpredicts the cross sections at the lowest energies by several orders of magnitude. These deviations are largest for systems involving the nuclei ^{100}Mo and ^{78}Kr. Figure 3 shows the data for ^{58}Ni and ^{64}Ni projectiles in comparison with coupled-channel calculations performed in the Rotating Frame Approximation[4]. These calculations include the effects of higher order couplings including one- and two-phonon excitations of low-lying 2^+ and 3^- states in projectile and target. The deformation parameters were taken from the literature. These calculations are in excellent agreement with the data for the systems involving ^{92}Mo and ^{86}Kr, but are unable to completely reproduce the measured cross sections for ^{58,64}Ni + ^{78}Kr and ^{100}Mo.

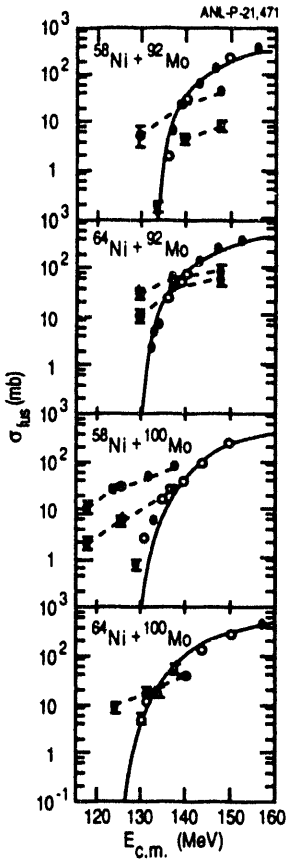

Figure 4: Comparison of the cross sections for one-and two-neutron transfer reactions (solid points) with the yields for evaporation residue production (open points) measured for the systems ^{58,64}Ni + ^{92,100}Mo. The solid lines for the fusion cross sections are the result of coupled-channels calculations. The dashed lines serve to guide the eye.

3.2 Influence of Transfer Reactions

In order to investigate whether couplings to other reaction channels (e.g. transfer reactions), or other nuclear structure effects are responsible for this discrepancy, few-nucleon transfer reactions have been measured for the Ni + Mo systems. The experiments were done with ^{92,100}Mo beams obtained from the positive-ion injector at ATLAS. Particle identification was achieved by detecting the Ni-like reaction products in inverse kinematics at forward angles in the focal plane of the split-pole spectrograph with a position sensitive Bragg detector. Details about the experimental setup can be found in Ref.[8]. In all cases neutron transfers are the dominant transfer reaction modes. The angle-and energy-integrated transfer cross sections for one-and two-neutron transfers are shown in Fig.4 together with the yields of the evaporation residues. The smallest transfer cross sections are observed for the systems ^{64}Ni + ^{100}Mo and ^{58}Ni + ^{92}Mo, i.e the most neutron-rich and neutron-deficient systems, re-

spectively. For the other systems, ^{64}Ni + ^{92}Mo and ^{58}Ni + ^{100}Mo, the transfer cross sections at energies close to the barrier are about of equal magnitude. This observation does not correlate with the deviation of the experimental fusion cross sections from the coupled-channels predictions. While for ^{58}Ni + ^{100}Mo discrepancies between the experimental and theoretical fusion cross sections are observed, the system ^{64}Ni + ^{92}Mo which shows about the same transfer yields, is quite well described by the coupled-channels calculations.

3.3 Influence of Nuclear Structure Effects

Since no clear correlation between sub-barrier fusion enhancement and the strength of the transfer cross sections has been observed for the Ni + Mo systems, the possible influence of other nuclear structure effects needs to be investigated. For the eight systems shown in Fig.3 good agreement between theory and experiment is observed for nuclei with a closed (N=50) neutron shell (^{92}Mo and ^{86}Kr), while the cross sections for the transitional nuclei ^{100}Mo and ^{78}Kr are underpredicted by the coupled-channels calculations.

The majority of systems for which sub-barrier fusion enhancement has been studied involve vibrational and rotational even-even nuclei. While the effects of deformation on fusion enhancement are well established, the influence of higher order vibrational modes on the fusion process is poorly understood. Vibrational nuclei are described by a Hamiltonian

$$H_\lambda = \frac{1}{2}\sum_{\lambda\mu} D_\lambda |\dot{\alpha}_{\lambda\mu}|^2 + \frac{1}{2}\sum_{\lambda\mu} C_\lambda |\alpha_{\lambda\mu}|^2 \qquad (1)$$

where D_λ and C_λ are the mass parameter and the restoring force parameter for the vibrational motion, respectively. For a $\lambda = 2$ vibration, C_2 depends on the excitation energy and the transition matrix element B(E2) via

$$C_2 = \frac{5}{2}\frac{E_{2^+}}{B(E2)} \cdot \left(\frac{3}{4\pi} Z e R^2\right)^2 \qquad (2)$$

The restoring force parameter C_2 is shown in Fig.5 as function of the mass A for even- even nuclei between A=28-150. Isotopes of various elements are connected by solid lines. The dashed line is the restoring force parameter calculated from the liquid drop model[9]. Clearly nuclear structure effects introduce huge variations in C_2, with closed shell nuclei (Ca, Zr, Sn) showing large values of C_2, while other nuclei (e.g. ^{78}Kr, ^{104}Ru and ^{124}Xe) have very small values of C_2.

Comparing the fusion cross sections measured in our experiments with the restoring force parameters C_2, an interesting correlation is observed. Systems involving 'stiff' nuclei with a large value of C_2 (^{86}Kr and ^{92}Mo) are well described by coupled-channel

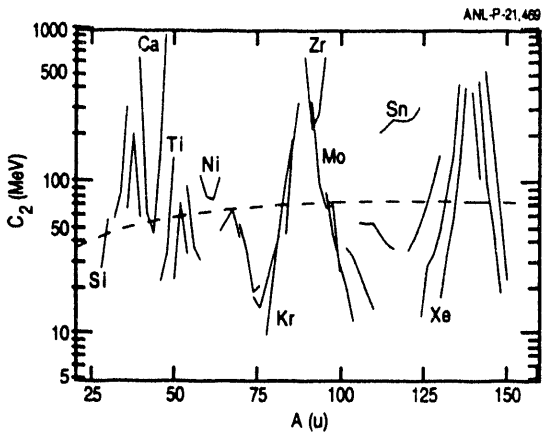

Figure 5: Restoring force parameter C_2 for even-even nuclei between A=28 -150. Isotopes for the various elements are connected by solid lines. The dashed line is the restoring force parameter calculated from the liquid drop model.

calculations which include one- and two-phonon excitations. Fusion reactions involving 'soft' nuclei , i.e. isotopes with a small C_2 (^{78}Kr and ^{100}Mo) show an additional fusion enhancement at sub-barrier energies. This additional enhancement is not reproduced by the present coupled-channels treatment indicating the need to include higher-order effects in the calculations. Similar correlations between softness and sub-barrier fusion enhancement have been observed for the systems[10] ^{46}Ti + ^{64}Ni and ^{50}Ti + ^{60}Ni.

4. Summary

Cross sections for evaporation residue production have been measured for the systems ^{58,64}Ni + ^{78,86}Kr and ^{58,64}Ni + ^{92,100}Mo using the gas-filled magnet technique. The excitation functions show strong sub-barrier fusion enhancements. Comparisons with coupled-channels calculations performed in the Rotating-Frame Approximations including one-and two- phonon excitations give excellent agreement for systems involving ^{86}Kr and ^{92}Mo nuclei while for ^{78}Kr and ^{100}Mo the experimental fusion yields at sub-barrier energies are still underpredicted by the calculations. The latter nuclei are transitional nuclei and in a vibrational description are 'soft', compared to 'stiff' closed shell nuclei. This observation points to a possible nuclear structure influence on the sub-barrier fusion enhancement which could be useful in cases where nuclei located outside the valley of β- stability are to be produced at low excitation energies with reasonably large cross sections.

This work was supported by the U. S. Department of Energy, Nuclear Physics Division under Contract No. W-31-109-ENG-38.

References

[1] M. Beckermann, Phys. Rep. **129**, (1985) 145

[2] S. G. Steadman and M. J. Rhoades-Brown, Annu. Rev. Nucl. Part. Sci. **36**, (1986) 649

[3] R. Vandenbosch, Annu. Rev. Nucl. Part. Sci. **42**, (1992) 447

[4] H. Esbensen and S. Landowne, Nucl Phys. **A492**, (1989) 473

[5] K. E. Rehm et al., Phys. Lett. **B317** (1993) 31

[6] J. E. Spencer and H. A. Enge, Nucl. Inst. Methods, **49**, (1967) 181

[7] K. E. Rehm et al. Nucl. Instr. and Meth. **A344** (1994) 614

[8] K. E. Rehm and F. L. H. Wolfs, Nucl. Instr. and Meth. **A 273** (1988) 282

[9] A. Bohr and B. Mottelson, Nuclear Structure Vol. II, Benjamin Inc. 1975

[10] A. M. Vinod Kumar et al., Contribution to this Conference

DATE
FILMED
9/29/94
END